Published OnlineFirst March 3, 2009; DOI: 10.1158/1535-7163.MCT-08-0656

Molecular imaging of Bcr-Abl phosphokinase in a xenograft model

Ji Yuan Wu,[1] David J. Yang,[2] Laura S. Angelo,[1] Saady Kohanim,[2] and Razelle Kurzrock[1]

[1]Department of Investigational Cancer Therapeutics (Phase I Program), Division of Cancer Medicine, and [2]Department of Experimental Diagnostic Imaging, The University of Texas M. D. Anderson Cancer Center, Houston, Texas

Abstract

The purpose of this study was to determine whether the Bcr-Abl tyrosine kinase can be assessed by γ-imaging using an ^{111}In-labeled anti-phosphotyrosine (APT) antibody, and if the response to treatment with imatinib could be detected using this imaging technique. APT antibody was labeled with ^{111}In using ethylenedicysteine (EC) as a chelator. To determine if ^{111}In-EC-APT could assess a nonreceptor tyrosine kinase, xenografts of the human chronic myelogenous leukemia cell line K562 were used. γ-Scintigraphy of the tumor-bearing mice, before and after imatinib treatment, was obtained 1, 24, and 48 h after they were given ^{111}In-EC-APT (100 μCi/mouse i.v.). ^{111}In-EC-APT is preferentially taken up by Bcr-Abl-bearing tumor cells when compared with ^{111}In-EC-BSA or ^{111}In-EC-IgG$_1$ controls and comparable with the level of uptake of ^{111}In-EC-Bcr-Abl. Imatinib treatment resulted in decreased expression of phospho-Bcr-Abl by Western blot analysis, which correlated with early (4 days after starting imatinib) kinase down-regulation as assessed by imaging using ^{111}In-EC-APT. The optimal time to imaging was 24 and 48 h after injection of ^{111}In-EC-APT. Although tumor regression was insignificant on day 4 after starting imatinib treatment, it was marked by day 14. ^{111}In-EC-APT can assess intracellular phosphokinase activity, and down-regulation of phosphokinase activity predates tumor regression. This technique may therefore be useful in the clinic to detect the presence of phosphokinase activity and for early prediction of response. [Mol Cancer Ther 2009;8(3):703–10]

Received 7/14/08; revised 1/2/09; accepted 1/19/09; published OnlineFirst 3/3/09.

Grant support: Supported by Clinical and Translational Science Award Number UL1RR024148 from the National Center For Research Resources. The content is solely the responsibility of the authors and does not necessarily represent the official views of the National Center For Research Resources or the National Institutes of Health.

The costs of publication of this article were defrayed in part by the payment of page charges. This article must therefore be hereby marked *advertisement* in accordance with 18 U.S.C. Section 1734 solely to indicate this fact.

Requests for reprints: Razelle Kurzrock, Department of Investigational Cancer Therapeutics (Phase I Program), Division of Cancer Medicine, The University of Texas M. D. Anderson Cancer Center, Unit 455, P.O. Box 301402, Houston, TX 77030. Phone: 713-794-1226; Fax: 713-563-0566. E-mail: rkurzroc@mdanderson.org

doi:10.1158/1535-7163.MCT-08-0656

Introduction

We are entering an age in which it may be feasible to use state-of-the-art imaging not only for the diagnosis of cancer and gauging the response to treatment, but also to determine which agents to use for therapy and to predict the potential for response based on early target modulation. For example, positron emission tomography using ^{18}F-fluorodeoxyglucose is widely used in clinical studies to identify metabolically active tumor cells. It is limited, however, by its nonspecificity, that is, it does not differentiate between types of tumors or at times between tumors and other inflammatory processes. Molecular imaging attempts to more specifically recognize protein targets, and one method of doing this exploits a homing agent bound to a radiotracer through a chelator, with the homing agent being a molecule that recognizes a protein specifically or preferentially expressed on cancer cells. Hence, imaging agents can be tailored to a specific malignancy based on the expression of cellular proteins, the availability of homing agents specific to that protein, and the availability of a chelator that can bind to the homing agent.

Recently, a few studies have begun to explore the possibility of receptor imaging using radiolabeled antibodies or bioluminescence nanotechnology directed against the receptor, or with the use of labeled ligands that interact with the receptor or with small-molecule tracers (1–8). Such imaging technology has been applied to epidermal growth factor receptor (EGFR), HER-2 receptor, vascular endothelial growth factor receptor, and TRAIL receptor in animal models (1–8). Apart from aberrant receptor tyrosine kinases, there are many other nonreceptor tyrosine kinases, including Src and Bcr-Abl, which when overexpressed or constitutively activated play a key role in the development of certain cancers. In addition, some of these tyrosine kinases are suppressed by small-molecule inhibitors, such as imatinib or dasatinib or others, which target the ATP-binding site in the tyrosine kinase domain (9–11). Indeed, there is a wealth of kinase inhibitors now entering clinical trials, and perhaps one of the most important questions in oncology today is how to predict which patients will respond to which kinase inhibitor. A noninvasive imaging technique that could detect the presence of the phosphorylated target and show early evidence of modulation by the drug administered would therefore be useful.

Antibodies are chosen for imaging studies based on the expression pattern of specific target molecules on the tumor cells. Following injection of radiolabeled antibodies, single-photon emission computed tomography (SPECT) images are taken at various time points to determine the optimal time to imaging after injection. This technique is noninvasive in contrast to biopsies, which contain sampling errors. Antibodies could also be used therapeutically if the antibody is linked to a radioablative molecule. The current

Published OnlineFirst March 3, 2009; DOI: 10.1158/1535-7163.MCT-08-0656

study uses ^{111}In-labeled anti-phosphotyrosine (APT) antibodies to image the Bcr-Abl tyrosine kinase in a tumor-bearing xenograft. The specific uptake of radiolabeled antibody by the tumor and changes in imaging after treatment with imatinib were determined.

Materials and Methods

Cell Lines

K562 is a chronic myelogenous leukemia (CML) blast crisis cell line expressing constitutively activated Bcr-Abl tyrosine kinase. K562 was purchased from the American Type Culture Collection. Cells were subcultured twice weekly in RPMI 1640 with 10% fetal bovine serum (Gemini Bio-Products) and maintained in a humidified incubator with 5% CO_2.

Antibodies and Reagents

Murine APT antibody 4G10 was purchased from Upstate Biotechnology and used at a dilution factor of 1:2,000. For Western blot analysis, murine anti-β-actin antibody was used as a control for protein loading (murine IgG_1; Sigma-Aldrich). The anti-Abl and anti-Bcr-Abl antibody 8E9 is from BD Biosciences. Anti-phospho-Bcr-Abl antibodies were obtained from Cell Signaling Technology. The murine IgG_1 and anti-phospho-Bcr-Abl antibodies were also used in the imaging portion of the study. Goat anti-rabbit or goat anti-mouse IgG heavy and light chain secondary antibody was purchased from Bio-Rad Laboratories. PEG-300 was purchased from Sigma-Aldrich, and imatinib was purchased from Novartis.

Western Blot Analysis

Western analysis was used to detect steady-state levels of phospho-Bcr-Abl proteins. Cells were collected, washed once with PBS, and lysed in solubilization buffer [40 mmol/L HEPES (pH 7.4), 150 mmol/L NaCl, 1.5 mmol/L $MgCl_2$, 1 mmol/L EGTA, 1 mmol/L EDTA, 100 mmol/L NaF, 10 mmol/L sodium pyrophosphate, 10% glycerol, 1% Triton X-100 plus protease inhibitors: 1 mmol/L phenylmethylsulfonyl fluoride, 1 mmol/L sodium vanadate, 10 μg/mL leupeptin, and 10 μg/mL aprotinin] for 30 min on ice. Total cell lysates were obtained after centrifugation at 14,000 rpm for 5 min. Protein concentration was measured using the BCA kit (Pierce Biotechnology), and 20 μg/lane protein was loaded onto an 8% SDS-PAGE gel. Proteins were transferred to nitrocellulose. The membrane was blocked with 3% bovine serum albumin (BSA) in TBS containing 0.1% Tween 20 for 1 h and then incubated with primary antibody in 3% BSA at room temperature for 2 h or at 4°C overnight. Blots were washed and then incubated with either goat anti-rabbit secondary antibody (1:3,000) or goat anti-mouse secondary antibody (1:4,000; Bio-Rad Laboratories) for 1 h and detected by enhanced chemiluminescence (Amersham Pharmacia Biotech). Blots were exposed to film (Kodak Biomax).

Preparation of ^{111}In-Ethylenedicysteine-APT

The antibodies were labeled with ^{111}In ($t_{1/2}$ = 2.805 days). ^{111}In isotope was selected to allow for a longer time observation. Ethylenedicysteine (EC) was selected as a chelator because EC-drug conjugates can be labeled with ^{111}In easily and efficiently with high radiochemical purity and stability (12–14). Synthesis of EC was prepared in a two-step manner as described (15, 16). EC was conjugated to APT antibody, murine IgG_1, anti-phospho-Bcr-Abl, or BSA using sulfo-*N*-hydroxysuccinimide and 1-ethyl-3-(3-dimethylaminopropyl) carbodiimide HCl as coupling agents. BSA was stirred with EC, sulfo-*N*-hydroxysuccinimide, and 1-ethyl-3-(3-dimethylaminopropyl) carbodiimide HCl at room temperature for 17 h. After dialysis, 2.3 to 3.4 mg EC antibody was obtained. ^{111}In was added into a vial containing EC antibody (0.1 mg) to yield ^{111}In-EC-BSA, ^{111}In-EC-IgG_1, ^{111}In-EC-Bcr-Abl, or ^{111}In-EC-APT. Radiochemical purity for EC antibodies (Rf = 0.1) were >95% as determined by radio-TLC (Bioscan) and labeled antibodies were eluted with saline or acetone.

Growth of K562 Tumors in Immunodeficient Mice

All animal work was approved by The University of Texas M. D. Anderson Institutional Animal Care and Use Committee. Six-week-old female Swiss nude mice were provided by the Department of Experimental Radiology (M. D. Anderson Cancer Center). Mice were housed in sterile filter-capped microisolator cages and provided with sterilized food and water. K562 cells (6×10^6)/100 μL/mouse were mixed with 50% Matrigel (BD Biosciences) in RPMI 1640 and injected s.c. into the right rear flank of the mouse. For the K562 tumor growth curve, a total of 10 mice were divided into two groups: a control group given vehicle alone and a group treated with imatinib. In the control group, 100 μL PEG-300 resuspended in sterile water was given by oral gavage; imatinib (100 mg/kg) was given to the mice in the experimental group in the same manner as the vehicle control was delivered. Treatment was initiated when the tumors were 0.3 cm in size. Body weight and tumor size were measured every other day until day 14 after treatment. Tumor size or volume was calculated as $V = (L \times W^2) \times 0.52$, where L is the length and W is the width of the xenograft. Mice were sacrificed and tumors were removed and minced. K562 tumor cells were lysed and the phosphorylation status of Bcr-Abl was assessed for both treatment and control groups.

Imaging of K562 (Bcr-Abl-Positive) Tumors in Immunodeficient Mice

K562 tumor-bearing mice were divided into three groups for the imaging portion of the study. Group I received ^{111}In-EC-BSA (n = 5). Group II received ^{111}In-EC-APT (n = 5). Group III also received ^{111}In-EC-APT monoclonal antibody (n = 5). Mice in groups I and II did not receive imatinib treatment. Mice in group III were treated with imatinib (100 mg/kg/d). Two additional groups of five mice were injected with either ^{111}In-EC-IgG_1 or ^{111}In-EC-Bcr-Abl antibody as negative and positive controls, respectively. The imaging portion of the study was initiated 3 days after the start of treatment. ^{111}In-labeled compound (100 μCi; ^{111}In-EC-BSA, ^{111}In-EC-IgG_1, ^{111}In-EC-Bcr-Abl, or ^{111}In-EC-APT) was injected through the tail vein. Imatinib treatment in group III continued throughout the imaging process. Scintigraphic images were acquired at 1, 2, 24, or 48 h following radiotracer injection using a γ-camera (M-camera; Siemens) equipped with a medium energy

Published OnlineFirst March 3, 2009; DOI: 10.1158/1535-7163.MCT-08-0656

collimator. This camera provides planar images. Regions of interest (counts per pixel) at the tumor lesion site and the symmetrical normal muscle site were used to determine tumor/muscle count density ratios. The ratios were used to compare the dynamic changes in the phosphorylation state of Bcr-Abl in the cytoplasm after imatinib treatment as well as a reflection of the uptake of labeled antibody by the cells (significance determined by Student's *t* test). To verify tumor size and phosphorylation status precisely, one mouse from each group was selected for SPECT-CT (Gamma Medica). The mice were anesthetized by inhalation of isofluorine with oxygen and scanned by CT first with 512 slides and then SPECT-CT with 32 frames. All the images were finally fused together using the Amira software (Mercury Computer Systems) for bony structures or the Amide software (Crump Institute for Molecular Imaging, University of California at Los Angeles School of Medicine) for soft-tissue analysis.

Results

^{111}In-Labeled APT Antibodies Are Exploitable for Imaging Bcr-Abl-Positive Xenografts

To determine whether APT antibodies can be exploited for assessing nonreceptor tyrosine kinase Bcr-Abl-positive tumors, K562 xenografts were injected with ^{111}In-labeled BSA or APT antibody. BSA serves as a marker of blood flow to the tumor. Thus, normal blood flow to the tumor versus specific uptake of ^{111}In-EC-APT can be visualized. EC was selected as a chelator for all radiotracers employed in this study. Nude mice were injected with K562 tumor cells and the tumors were allowed to grow to 0.3 cm in diameter. Mice in the imatinib-treated group began therapy 3 days before the injection of ^{111}In-labeled antibodies and continued treatment during antibody injection for a total of 4 or 5 days of treatment for the imaging portion of the study. SPECT-CT images acquired 48 h after injection of ^{111}In-EC-BSA or ^{111}In-EC-APT are shown in Fig. 1. The tumor is indicated by arrows. Injection of ^{111}In-EC-APT antibody results in increased tumor uptake compared with injection of control ^{111}In-EC-BSA as determined by enhanced tumor-to-nontumor count density ratios (see Supplementary Data for three-dimensional movie file).[3]

To verify tumor size and phosphorylation status precisely, one mouse from each group was selected for SPECT-CT. Images were fused together using the Amira software, which allows visualization of bony structures in three dimensions (Fig. 1). SPECT-CT is a dynamic imaging process that combines functional and structural elements. Thus, SPECT-CT shows the structure of the organism and the location of the tumor and also detects the radioactive density of a specific area using computer software to enhance the image. Treatment with imatinib resulted in decreased uptake by the tumor of ^{111}In-EC-APT (Fig. 1). Coronal SPECT-CT was also used to visualize the amount of ^{111}In-EC-APT taken up by the tumor (Fig. 2). The difference between these images and the ones showing the bony structure (Fig. 1) is the software used to analyze the image. The Amide software was used to analyze soft-tissue uptake of the radiotracer in the coronal images (Fig. 2). The tumor is indicated by arrows. ^{111}In-EC-APT-injected mice show increased signal from the tumor compared with ^{111}In-EC-BSA-injected mice. Mice treated with imatinib for a total of 5 days exhibit decreased tumor signal (Fig. 2).

Unlike SPECT-CT, planar imaging is static and two-dimensional. Planar images are taken on a flat surface and can be used to measure the uptake of radiolabeled antibodies by the tumor in comparison with normal surrounding tissue. Regions of interest (counts per pixel) at the tumor lesion site and the symmetrical normal muscle site were used to determine tumor/muscle count density ratios. Scintigraphic images were taken 2, 24, or 48 h following radiolabeled antibody injection. A comparison of the uptake of all radiolabeled compounds is shown in Fig. 3A. K562 xenografts were injected with ^{111}In-EC-BSA, ^{111}In-EC-IgG$_1$, ^{111}In-EC-APT, or ^{111}In-EC-Bcr-Abl. ^{111}In-labeled IgG$_1$ and BSA were used as negative controls, whereas ^{111}In-EC-Bcr-Abl was used as a positive control. Both negative control molecules had decreased tumor/muscle ratios when compared with either ^{111}In-EC-APT or ^{111}In-EC-Bcr-Abl (tumor/muscle ratio: BSA = 1.5, IgG$_1$ = 1.9, APT = 4.0, and Bcr-Abl = 6.1) at the 48 h time point when uptake was the greatest (Fig. 3A and B).

Imatinib Treatment of K562 (Bcr-Abl-Positive) Xenografts Results in Decreased Tumor Volume and Decreased Expression of Phospho-Bcr-Abl by Western Blot Analysis

The effect of imatinib on K562 tumor growth was determined by calculating the tumor volume for mice treated with vehicle (PEG-300) or imatinib (100 mg/kg). For the K562 tumor growth curve, a total of 10 mice were divided into two groups: a control group given vehicle alone and a group treated with imatinib. In the control group, 100 μL vehicle resuspended in sterile water was given by oral gavage daily. Imatinib (100 mg/kg) was given to the mice in the experimental group in the same manner as the vehicle control was delivered. Body weight and tumor size were measured every other day until day 14 after treatment. An increase (235%) in tumor volume was seen in the mice treated with vehicle (top) when compared with the mice treated with imatinib (87% decrease; bottom) over the same 14-day period (Fig. 4A).

Levels of phospho-Bcr-Abl were analyzed by Western blot analysis to verify the anti-kinase effect of imatinib on Bcr-Abl in the xenografts. After tumor growth reached 0.3 cm, vehicle or imatinib was administered to the mice for 14 days. Mice were sacrificed and tumors were removed and minced. Cells were lysed and the phosphorylation status of Bcr-Abl was assessed for both treatment and control groups by Western blot analysis (Fig. 4B). Three different pairs of mice were analyzed for the expression of phospho-Bcr-Abl and phospho-Abl in the presence or absence of imatinib.

[3] Supplementary material for this article is available at Molecular Cancer Therapeutics Online (http://mct.aacrjournals.org/).

Published OnlineFirst March 3, 2009; DOI: 10.1158/1535-7163.MCT-08-0656

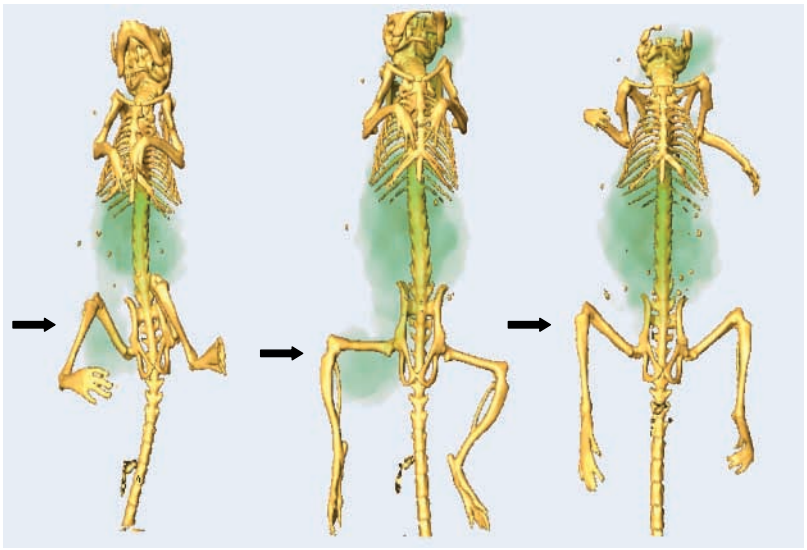

Figure 1. 48 h isosurface snap of SPECT-CT images comparing K562 tumor-bearing nude mice injected with ^{111}In-EC-BSA or ^{111}In-EC-APT before and after 5 d of imatinib treatment. Images were fused together using the Amira software, which allows visualization of bony structures in three dimensions. *Left,* imaged with ^{111}In-EC-BSA shows baseline levels of blood flow to the tumor (right leg); *middle,* imaged with ^{111}In-EC-APT detects the phosphokinase; *right,* imaged with ^{111}In-EC-APT after 5 d of imatinib shows down-regulation of the phosphokinase. Previous experiments have shown that radiolabeled isotypic control antibody does not image (8).

Phospho-Bcr-Abl and phospho-Abl levels are decreased following treatment with imatinib for 14 days in each of the xenografts studied. Total levels of Bcr-Abl and Abl protein remain unchanged following imatinib treatment. The K562 cell line was used as a positive control for the effect of imatinib (data not shown), and β-actin was used as a loading control (Fig. 4B).

Planar Imaging Shows a Higher Tumor/Muscle Ratio for ^{111}In-EC-APT and a Decrease in Tumor Uptake of Radiolabeled Antibody following Treatment with Imatinib at 24 and 48 h Post-Injection

Scintigraphic images were taken 24 or 48 h following radiolabeled antibody injection. Tumor/muscle count density ratios were used to compare the dynamic changes in the phosphorylation state of Bcr-Abl in the cytoplasm after imatinib treatment and also as a reflection of the uptake of labeled antibody by the cells. Mice in the imatinib-treated group began therapy 3 days before the injection of ^{111}In-EC-APT and continued treatment during antibody injection for a total of either 4 days (24 h imaging) or 5 days (48 h imaging) of treatment. Representative scintigraphic imaging of ^{111}In-labeled compounds in K562 xenografts are shown in Fig. 5A. The computer outlined region of interest shows higher tumor/muscle ratios as a function of time in ^{111}In-EC-APT-injected mice compared with ^{111}In-EC-BSA-injected mice (Fig. 5A and B). Decreased

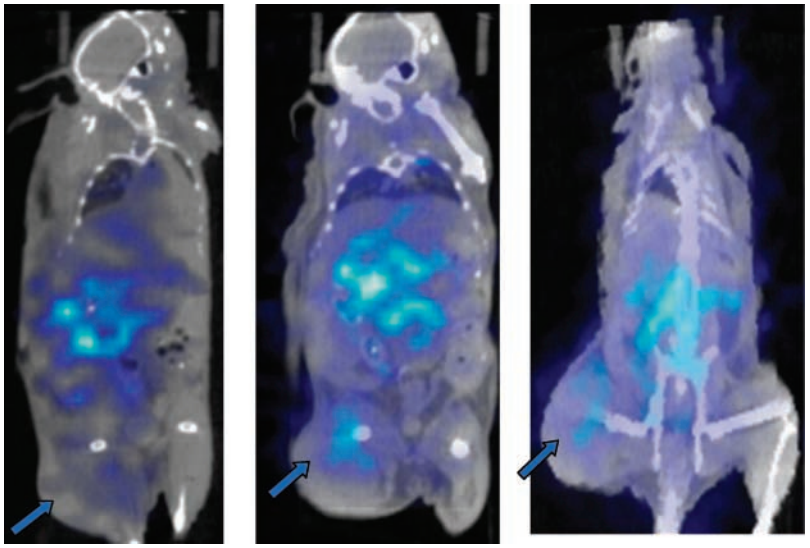

Figure 2. 48 h comparison of coronal SPECT-CT images of ^{111}In-EC-BSA-injected or ^{111}In-EC-APT-injected nude mice before and after 5-d imatinib therapy. Amide software was used for soft-tissue analysis. *Left,* imaged with ^{111}In-EC-BSA show baseline levels of blood flow to the tumor (right leg); *middle,* imaged with ^{111}In-EC-APT detects the phosphokinase; *right,* imaged with ^{111}In-EC-APT after 5 d of imatinib shows down-regulation of phosphokinase.

Published OnlineFirst March 3, 2009; DOI: 10.1158/1535-7163.MCT-08-0656

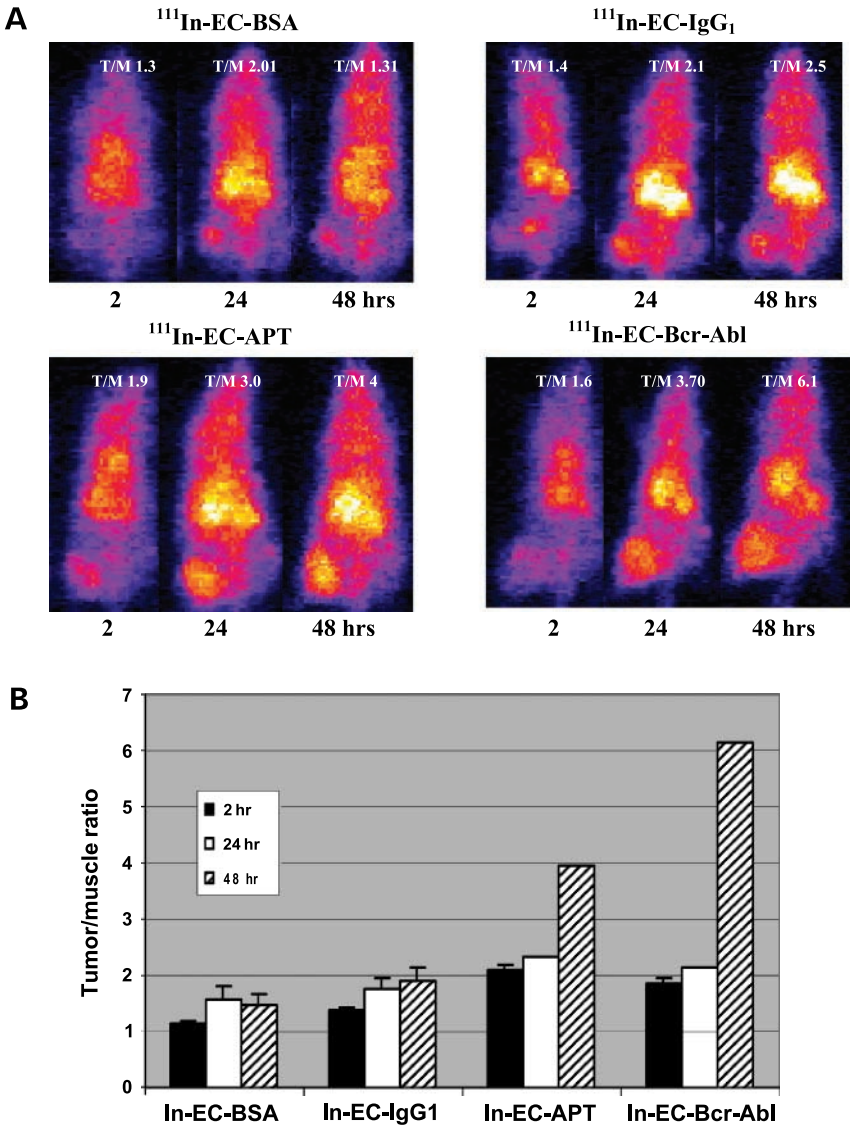

Figure 3. **A,** comparison of uptake of different radiolabeled compounds into K562 xenografts. Planar images of K562 xenografts were taken 2, 24, or 48 h after injection of ^{111}In-EC-BSA, ^{111}In-EC-IgG$_1$, ^{111}In-EC-APT, or ^{111}In-EC-Bcr-Abl. Scintigraphic images were acquired following radiotracer injection using a γ-camera equipped with a medium energy collimator. **B,** average tumor/muscle count density ratios of ^{111}In-EC-BSA, ^{111}In-EC-IgG$_1$, ^{111}In EC-APT, and ^{111}In-EC-Bcr-Abl regions of interest (counts per pixel) at the tumor lesion site and the symmetrical normal muscle site were used to determine tumor/muscle count density ratios 2, 24, and 48 h after injection of ^{111}In-labeled antibodies. Xenografts injected with ^{111}In EC-APT and ^{111}In-EC-Bcr-Abl had higher tumor/muscle count density ratios than mice injected with radiolabeled BSA or IgG$_1$, most notably at 48 h post-injection.

tumor/muscle ratios were detected by scintigraphic imaging in the imatinib-treated mice at 24 and 48 h post-injection ($P < 0.05$; Fig. 5B). Mice treated with vehicle alone showed no decrease in Bcr-Abl phosphorylation by scintigraphic imaging (data not shown). Images were also taken at 1 h post-injection, but uptake of radiolabeled antibodies was not evident at this time (data not shown). These results indicate that ^{111}In-EC-APT antibodies are preferentially taken up by the tumor cells and also that intracellular tyrosine kinases can be visualized with APT antibodies, and the response to imatinib can be visualized within 4 days of the start of treatment.

Discussion

Although kinase inhibitor treatment is proven successful in the clinic, the greatest challenge lies in predicting which patients will respond to this therapy. Traditional techniques used to predict patient responses to therapy include biopsies, which are invasive, painful, and potentially dangerous. In addition, data obtained from biopsies vary within the same patient and can therefore be unreliable. The development of novel imaging agents and techniques that would facilitate the prediction of responses to therapy is of paramount importance. The imaging technique presented here is potentially applicable to the clinic in that our experiments suggest that it allows assessment of the expression of the target molecule (constitutively phosphorylated tyrosine residues), and the effect of the kinase inhibitor on the target, in an animal model.

SPECT-CT provides target-specific cellular-based imaging findings. Other techniques used to monitor response include fluorescent *in situ* hybridization, quantitative PCR for Bcr-Abl, and assessment of phospho-CrkL. These techniques are valuable but may be limited by sampling errors. SPECT-CT images provide real-time dynamic

Published OnlineFirst March 3, 2009; DOI: 10.1158/1535-7163.MCT-08-0656

macroscopic whole-body biodistribution of a radiolabeled antibody. It can accurately quantify the tumor volume via CT attenuation correction. SPECT-CT, although expensive when compared with other methods of Bcr-Abl assessment, offers the advantage of seeing the result of treatment at an earlier stage (Western blot = 14 days for inhibition of Bcr-Abl; tumor volume = 14 days; imaging = 4 days) and can help predict for response by measuring levels of kinase activity before treatment. Also, it offers a noninvasive way to assess the effectiveness of treatment.

Previous studies by our group using anti-EGFR antibody (C225), anti-TRAIL death receptor 4 and 5 antibodies, and anti-17β-estradiol antibodies show the potential for these novel imaging techniques to detect their targets (1, 8, 17). In addition, our group has shown that APT antibody detects the phosphorylation of frequently overexpressed or constitutively activated tyrosine kinase receptors such as EGFR. These antibodies can identify which tumors bear the target molecule and show early EGFR phosphokinase down-regulation before that predicted for tumor response *in vivo* using a mouse model.[4]

The present study examines the potential use of radiolabeled APT antibodies to image tumors overexpressing an intracellular phosphotyrosine molecule. To our knowledge, this is the first use of an APT antibody to visualize an intracellular (nonreceptor) kinase phosphorylated on tyrosine and to successfully image the tumor after treatment with the kinase inhibitor imatinib.

The mechanism of entry of ^{111}In-EC-APT into the cell is dependent on the cellular target and the chelator. EC is the most recent and successful example of N_2S_2 chelates (18–21). EC can be labeled with metallic isotopes easily and efficiently with high radiochemical purity and stability (12–14). Certain antibodies (e.g., anti-EGFR and anti-carcinoembryonic antigen) bind to antigen and can be internalized through the endocytotic process (22–24). Endocytosis occurs through either specific enzymatic involvement or specific protein domains. Our biodistribution studies show internalization of the APT antibody. This internalization might be due to antigen-antibody-mediated induction of translocated protein following attachment to the host cell at the site of entry and is associated with the endocytotic process. Additionally, K562 cells express the FcγRIIa receptor exclusively (25), which binds to all IgG subclasses. This Fc receptor may contribute to radiolabeled antibody uptake; however, antigen specificity may be more important as evidenced by the high tumor/muscle ratios seen in ^{111}In-EC-Bcr-Abl-injected xenografts. Further study is warranted to evaluate which domain of the APT antibody is required for endocytosis. We have used this strategy previously to successfully image angiogenesis by EC-endostatin (26), EGFR (1, 27), apoptosis by EC-Annexin V (20), and TRAIL (death) receptor by EC-ETR1 and EC-ETR2 antibodies (8).

CML is a myeloproliferative disorder, whose dominant oncogenic product is the Bcr-Abl nonreceptor tyrosine kinase. Bcr-Abl resides in the cytoplasm and drives CML and Philadelphia chromosome-positive acute lymphocytic leukemia growth (9). Targeting Bcr-Abl kinase activity results in dramatic responses in the clinic (10, 11). Although CML is not typically a solid tumor, chloromas are extramedullary tumor nodules that can occur in this type of leukemia (28). It is conceivable that chloromas could be visualized by this technique. The transduction-transplantation model of CML could also be explored in the future to more thoroughly investigate the use of this technique in CML (29). More importantly, our model shows the potential for our imaging technique to detect an intracellular kinase. Many oncogenic kinases are intracellular, and because even receptor kinases are phosphorylated on their intracellular domains, our results support the potential for such imaging to be applied in the clinical setting.

Our experiments showed that down-regulation of Bcr-Abl kinase could be shown by imaging after only 4 days of treatment with imatinib (Fig. 5A), a point at which there is negligible change in growth (Fig. 4A). Although tyrosine

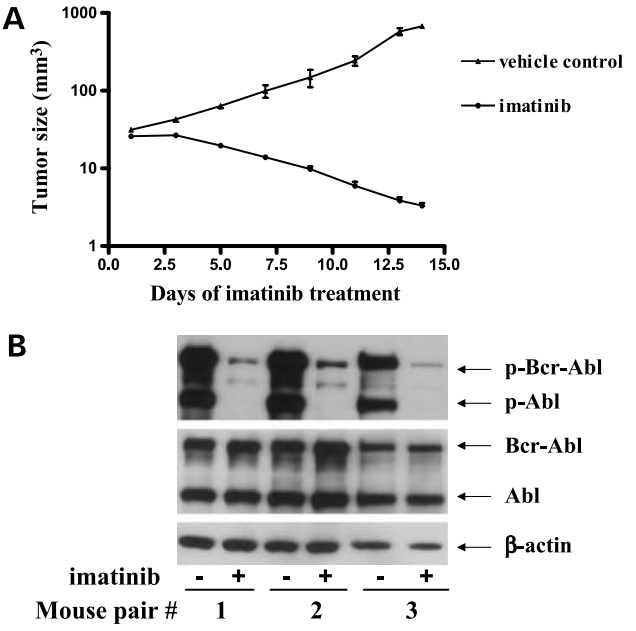

Figure 4. **A,** comparison of tumor volume in K562 xenografts with or without imatinib treatment for 14 d. In the control group, 100 μL PEG-300 resuspended in sterile water was given by oral gavage daily; imatinib (100 mg/kg) was given to the mice in the experimental group in the same manner as the vehicle control was delivered. Both control treated and imatinib-treated mice started with tumors of ~0.3 cm in diameter. Tumor size was measured every other day until day 14 after treatment. Tumor regression in the imatinib-treated mice is negligible to mild during the first week but marked by day 14. Tumors grow significantly in the vehicle control-treated mice. **B,** Western blot showing changes in Bcr-Abl and Abl protein phosphorylation in three pairs of K562-bearing xenografts with or without imatinib treatment for 14 d. Anti-β-actin antibody was used as a control for protein loading. Steady-state levels of phospho-Bcr-Abl and Abl but not total Bcr-Abl or Abl are significantly decreased on day 14.

[4] Gong et al., submitted for publication.

Published OnlineFirst March 3, 2009; DOI: 10.1158/1535-7163.MCT-08-0656

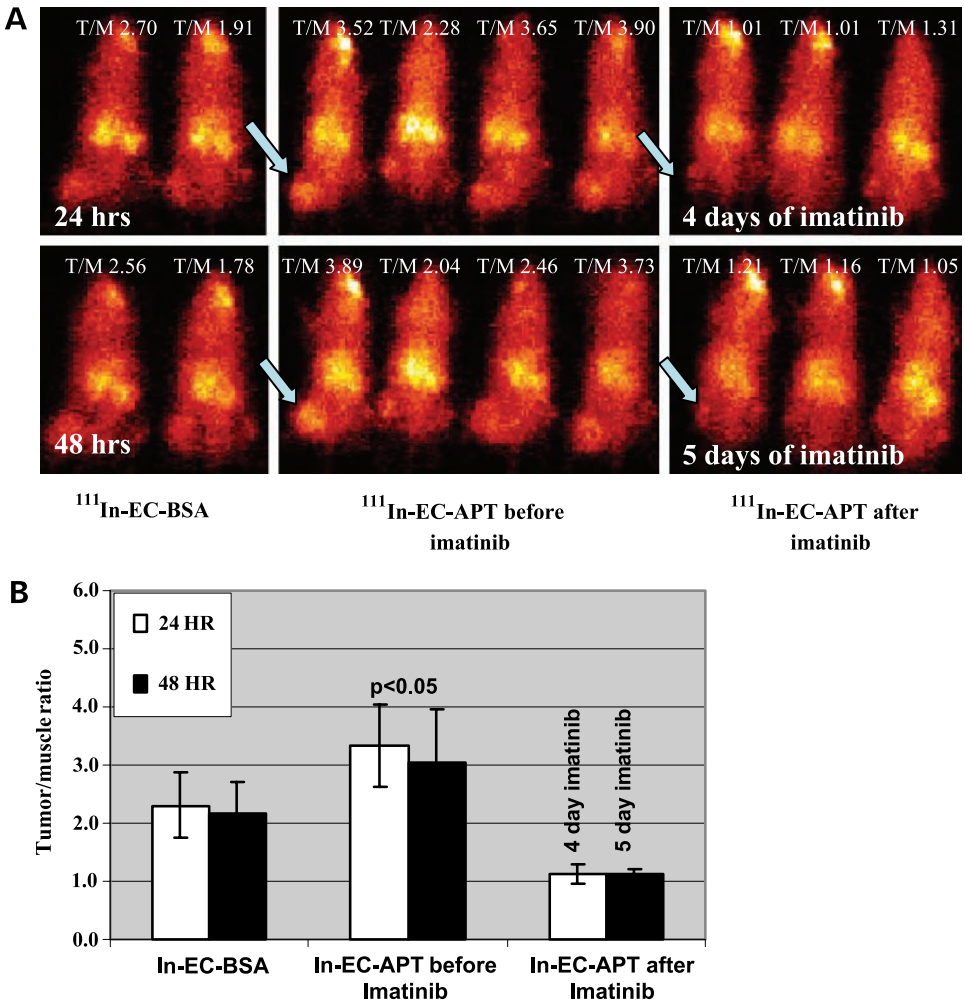

Figure 5. **A,** Planar images of K562 xenografts 24 or 48 h after injection of ^{111}In-EC-BSA or ^{111}In-EC-APT before and after 4 or 5 d of imatinib treatment. **B,** average tumor/muscle count density ratios of ^{111}In-EC-BSA and ^{111}In EC-APT before and after 4 or 5 d of imatinib therapy of K562 xenografts (n = 5 in each group) 24 and 48 h after injection of ^{111}In-labeled antibodies. Mice injected with ^{111}In-EC-APT had higher tumor/muscle count density ratios than mice treated with ^{111}In-EC-BSA ($P < 0.05$). Furthermore, after treatment with 4 or 5 d of imatinib, respectively, tumor/muscle count density ratios are markedly decreased ($P < 0.05$, Student's t test).

kinases other than Bcr-Abl would be detected by our imaging antibody, it is known that the predominant phosphokinase down-regulated by imatinib in K562 CML cells is Bcr-Abl, and this is consistent with our Western blot data (Fig. 4B). Clear regression of tumor occurred later (Fig. 4A). Therefore, the imaging results were able to predict tumor response. Although cell death may account for some of the shutdown in kinase imaging, it is unlikely to account for the dramatic results seen so early after imatinib treatment, especially in light of lack of tumor regression at that point. Hence, it is worthwhile to study the ability of imaging agents such as ^{111}In-EC-APT to detect baseline levels of phosphokinase in patients and also for the initial selection of a specific kinase inhibitor as treatment. The latter could be accomplished by using specific APT antibody-based imaging agents such as anti-phospho-Kit or anti-phospho-EGFR to establish the presence of the target kinase before treatment with a Kit or EGFR kinase inhibitor, respectively. Furthermore, detection of kinase down-regulation after only a few days of therapy could be studied as a potential early predictor of response in the clinical setting.

Disclosure of Potential Conflicts of Interest

No potential conflicts of interest were disclosed.

References

1. Schechter NR, Yang DJ, Azhdarinia A, et al. Assessment of EGF receptors with 99mTc ethylenedicysteine-C225 monoclonal antibody. Anti Cancer Drugs 2003;14:49 – 56.

2. Kramer-Marek G, Kiesewetter DO, Martiniova L, Jagoda E, Lee SB, Capala J. [(18)F]FBEM-Z (HER2:342)-Affibody molecule—a new molecular tracer for *in vivo* monitoring of HER2 expression by positron emission tomography. Eur J Nucl Med Mol Imaging 2008;35:1008 – 18.

3. Takahashi N, Yang DJ, Kohanim S, et al. Targeted functional imaging of estrogen receptors with 99mTc-GAP-EDL. Eur J Nucl Med Mol Imaging 2007;34:354 – 62.

4. Cai W, Niu G, Chen X. Multimodality imaging of the HER-kinase axis in cancer. Eur J Nucl Med Mol Imaging 2008;35:186 – 208.

5. Welsher K, Liu Z, Daranciang D, Dai H. Selective probing and imaging of cells with single walled carbon nanotubes as near-infrared fluorescent molecules. Nano Lett 2008;8:586 – 90.

6. Cai W, Chen X. Multimodality imaging of vascular endothelial growth factor and vascular endothelial growth factor receptor expression. Front Biosci 2007;12:4267 – 79.

7. Pai A, Giekas A, Doubrovin M, et al. Molecular imaging of EGFR kinase activity in tumors with ^{124}I-labeled small molecular tracer and positron emission tomography. Mol Imaging Biol 2006;8:262 – 77.

Published OnlineFirst March 3, 2009; DOI: 10.1158/1535-7163.MCT-08-0656

8. Gong J, Yang DJ, Kohanim S, Humphreys R, Broemeling L, Kurzrock R. Novel *in vivo* imaging shows up-regulation of death receptors by paclitaxel and correlates with enhanced antitumor effects of receptor agonist antibodies. Mol Cancer Ther 2006;5:2991 – 3000.

9. Kurzrock R, Shtalrid M, Romero P, et al. c-abl protein product in Philadelphia-positive acute lymphoblastic leukaemia. Nature 1987;325:631 – 5.

10. Talpaz M, Shah NP, Kantarjian H, et al. Dasatinib in imatinib-resistant Philadelphia chromosome-positive leukemias. N Engl J Med 2006;354: 2531 – 41.

11. Druker BJ, Sawyers CL, Kantarjian H, et al. Activity of a specific inhibitor of the BCR-ABL tyrosine kinase in the blast crisis of chronic myeloid leukemia and acute lymphoblastic leukemia with the Philadelphia chromosome. N Engl J Med 2001;344:1038 – 42.

12. Blondeau P, Berse C, Gravel D. Dimerization of an intermediate during the sodium in liquid ammonia reduction of l-thiazolidine-4-carboxylic acid. Cancer J Chem 1967;45:49 – 52.

13. Van Nerom CG, Bormans GM, De Roo MJ, Verbruggen AM. First experience in healthy volunteers with Tc-99m-L-ethylenedicysteine, a new renal imaging agent. Eur J Nucl Med 1993;20:738 – 46.

14. Surma MJ, Wiewiora J, Liniecki J. Usefulness of Tc-99m-*N,N*-ethylene-1-dicysteine complex for dynamic kidney investigations. Nucl Med Commun 1994;15:628 – 35.

15. Ilgan S, Yang DJ, Higuchi T, et al. 99mTc-Ethylenedicysteine-folate: a new tumor imaging agent: synthesis, labeling, and evaluation in animals. Cancer Biother Radiopharm 1998;13:427 – 35.

16. Zareneyrizi F, Yang DJ, Oh CS, et al. Synthesis of 99mTc ethylenedicysteine colchicine for evaluation of anti-angiogenic effect. Anti Cancer Drugs 1999;10:685 – 92.

17. Takahashi N, Yang DJ, Kurihara H, et al. Functional imaging of estrogen receptors with radiolabeled-GAP-EDL in rabbit endometriosis model. Acad Radiol 2007;14:1050 – 7.

18. Yang D, Yukihiro M, Yu DF, et al. Assessment of therapeutic tumor response using 99mTc-ethylenedicysteine-glucosamine. Cancer Biother Radiopharm 2004;19:443 – 56.

19. Yang DJ, Kim C-G, Schechter NR, et al. Imaging with 99mTc-EC-DG targeted at the multifunctional glucose transport system: feasibility study with rodents. Radiology 2003;226:465 – 73.

20. Yang DJ, Azhdarinia A, Wu P, et al. *In vivo* and *in vitro* measurement of apoptosis in breast cancer cells using 99mTc-EC-Annexin V. Cancer Biother Radiopharm 2001;16:73 – 83.

21. Yang DJ, Ozaki K, Oh CS, et al. 99mTc-EC-guanine: synthesis, biodistribution, and tumor imaging in animals. Pharmaceutical Res 2005;22: 1471 – 9.

22. Perera RM, Zoncu R, Johns TG, et al. Internalization, intracellular trafficking, and biodistribution of monoclonal antibody 806: a novel anti-epidermal growth factor receptor antibody. Neoplasia 2007;9: 1099 – 110.

23. Schmidt MM, Thurber GM, Wittrup KD. Kinetics of anti-carcinoembryonic antigen antibody internalization: effects of affinity, bivalency, and stability. Cancer Immunol Immunother 2008. Epub ahead of print.

24. Avignolo C, Bagnasco L, Biasotti B, et al. Internalization via Antennapedia protein transduction domain of an scFv antibody toward c-Myc protein. FASEB J 2008;22:1237 – 45.

25. Allhorn M, Olin AI, Nimmerjahn F, Collin M. Human IgG/FccR interactions are modulated by streptococcal IgG glycan hydrolysis. PLoS ONE 2008;3:e1413.

26. Yang DJ, Kim KD, Schechter NR, et al. Assessment of anti-angiogenic effect using 99mTc-EC-endostatin. Cancer Biother Radiopharm 2002;17: 233 – 45.

27. Schechter NR, Wendt RE III, Yang DJ, et al. Radiation dosimetry of 99mTc-labeled C225 in patients with squamous cell carcinoma of the head and neck. J Nucl Med 2004;45:1683 – 7.

28. Fritz J, Vogel W, Bares R, Horger M. Radiologic spectrum of extramedullary relapse of myelogenous leukemia in adults. AJR Am J Roentgenol 2007;189:209 – 18.

29. Cuiffo B, Ren R. Models of hematopoietic malignancies: chronic myeloid leukemia. Drug Discov Today Dis Models 2006;3:183 – 9.

AACR American Association for Cancer Research

Molecular Cancer Therapeutics

Molecular imaging of Bcr-Abl phosphokinase in a xenograft model

Ji Yuan Wu, David J. Yang, Laura S. Angelo, et al.

Mol Cancer Ther 2009;8:703-710. Published OnlineFirst March 3, 2009.